Eur. Phys. J. A (2015) **51**: 90
DOI 10.1140/epja/i2015-15090-3

THE EUROPEAN PHYSICAL JOURNAL A

Letter

Important influence of single neutron stripping coupling on near-barrier ^{8}Li + ^{90}Zr quasi-elastic scattering

A. Pakou[1,a], N. Keeley[2,b], D. Pierroutsakou[3], M. Mazzocco[4,5], L. Acosta[6,7], X. Aslanoglou[1], A. Boiano[3], C. Boiano[8], D. Carbone[9], M. Cavallaro[9], J. Grebosz[10], M. La Commara[11,3], C. Manea[5], G. Marquinez-Duran[12], I. Martel[12], C. Parascandolo[3], K. Rusek[13], A.M. Sánchez-Benítez[14], O. Sgouros[1], C. Signorini[15], F. Soramel[4,5], V. Soukeras[1], E. Stiliaris[16], E. Strano[4,5], D. Torresi[4,5], A. Trzcińska[13], Y.X. Watanabe[17], and H. Yamaguchi[18]

[1] Department of Physics and HINP, The University of Ioannina, 45110 Ioannina, Greece
[2] National Centre for Nuclear Research, ul. Andrzeja Sołtana 7, 05-400, Otwock, Poland
[3] INFN, Sezione di Napoli, via Cintia, 80126 Napoli, Italy
[4] Dipartimento di Fisica e Astronomia, Università di Padova, via Marzolo 8, I-35131, Padova, Italy
[5] INFN, Sezione di Padova, via Marzolo 8, I-35131, Padova, Italy
[6] Instituto de Fisica, Universidad Nacional Autonoma de Mexico, Mexico D. F. 01000, Mexico
[7] INFN, Sezione di Catania, via S. Sofia 64, 95125, Catania, Italy
[8] INFN, Sezione di Milano, via Celoria 16, I-20133 Milano, Italy
[9] INFN Laboratori Nazionali del Sud, via S. Sofia 62, 95125, Catania, Italy
[10] The Henryk Niewodniczański Institute of Nuclear Physics (IFJ PAN), Krakow, Poland
[11] Dipartimento di Scienze Fisiche, Università di Napoli “Federico II”, via Cintia, I-80126 Napoli, Italy
[12] Departamento de Fisica Aplicada, Universidad de Huelva E-21071 Huelva, Spain
[13] Heavy Ion Laboratory, University of Warsaw, Pasteura 5a, 02-093, Warsaw, Poland
[14] Centro de Física Nuclear da Universidade de Lisboa, 1649-003 Lisboa, Portugal
[15] INFN, LNL, viale dell'Università 2, I-35020 Legnaro, Italy
[16] Institute of Accelerating Systems and Applications and Department of Physics, University of Athens, Greece
[17] Institute of Particle and Nuclear Studies (IPNS), High Energy Accelerator Research Organization (KEK), Tsukuba, 305-0801 Ibaraki, Japan
[18] Center for Nuclear Study (CNS), University of Tokyo, RIKEN campus, 2-1 Hirosawa, Wako, Saitama 351-0198, Japan

Received: 29 June 2015
Published online: 29 July 2015

Communicated by N. Alamanos

Abstract. Quasi-elastic scattering data were obtained for the radioactive nucleus ^{8}Li on a ^{90}Zr target at the near-barrier energy of 18.5 MeV over the angular range $\theta_{\rm lab} = 15^\circ$ to 80°. They were analyzed within the coupled channels and coupled reaction channels frameworks pointing to a strong coupling effect for single neutron stripping, in contrast to ^{6,7}Li + ^{90}Zr elastic scattering at similar energies, a non-trivial result linked to detailed differences in the structure of these Li isotopes.

1 Introduction

The effect of breakup and/or transfer couplings on elastic scattering of weakly bound nuclei at near-barrier energies has recently become the subject of considerable research effort, see *e.g.* [1] and references therein. This effort has so far concentrated on radioactive nuclei such as ^{6,8}He, ^{11}Be and ^{11}Li and the stable weakly bound nuclei ^{6,7}Li and ^{9}Be. Large transfer/breakup cross sections persist to very low energies —even below the barrier— for light weakly bound projectiles on heavy [2], medium [3] and light targets [4,5], although a large cross section for a given reaction channel or set of channels is not always a reliable guide to the importance of its coupling effect on the elastic scattering [6–12]. The radioactive ^{8}Li nucleus has been less investigated, both experimentally and theoretically. This nucleus presents an interesting test case in comparison with its stable but weakly bound neighbours ^{6,7}Li. It has a threshold of 2.03 MeV for $^{8}\mathrm{Li} \to {}^{7}\mathrm{Li} + n$ breakup compared to 1.47 MeV for $^{6}\mathrm{Li} \to \alpha + d$ and 2.47 MeV for $^{7}\mathrm{Li} \to \alpha + t$ breakup; the single neutron separation thresholds, $S_{\rm n}$, are 2.03 MeV, 7.25 MeV and 5.66 MeV for ^{8}Li, ^{7}Li and ^{6}Li, respectively, providing an interesting possibility of comparing the interplay of breakup and transfer couplings effects over a range of Q values without the complication of significant differences in Coulomb barriers.

[a] e-mail: apakou@cc.uoi.gr (Corresponding author)
[b] e-mail: nicholas.keeley@ncbj.gov.pl

Beams of ^{8}Li at near-barrier energies can be obtained at small facilities with the in flight technique, *e.g.*, TwinSol at The University of Notre Dame [13] and recently the EXOTIC facility at the Laboratori Nationali di Legnaro [14] and the RIBRAS facility at the University of São Paulo [15]. Several studies of data from TwinSol have appeared in the literature, *e.g.*, refs. [16,17], and a comprehensive study of ^{8}Li on ^{208}Pb at near-barrier energies is given in ref. [18] where the elastic scattering as well as substantial ^{7}Li production due to breakup and/or transfer were measured. The results were analyzed in ref. [19] via coupled channels Born approximation and coupled reaction channels (CRC) methods, concluding that the ^{7}Li yield comes predominantly from the one-neutron stripping channels which also have a significant coupling effect on the elastic scattering.

In this work we present new ^{8}Li quasi-elastic scattering data for a medium mass target, ^{90}Zr. Particular care was taken to obtain as many points as possible in the region of the Coulomb-nuclear interference peak. CRC calculations find a strong coupling effect due to single neutron stripping, similar to that found in the ^{8}Li + ^{208}Pb system, in contrast to the ^{6,7}Li + ^{90}Zr systems. We therefore find that the significant coupling effect due to single neutron stripping persists for ^{8}Li scattered from a medium mass target and, unlike ^{6}Li + ^{90}Zr at a similar incident energy, a satisfactory description of the ^{8}Li data may be obtained without including breakup couplings.

2 Experimental details and data reduction

A description of the experiment was given in ref. [20] and we give further details here. The ^{8}Li secondary beam was produced at the EXOTIC facility [14,21] of the Laboratori Nazionale di Legnaro (LNL), Italy by means of the in flight (IF) technique and the ^{2}H(^{7}Li, ^{8}Li)p reaction ($Q = -0.19$ MeV) with a ^{7}Li^{+3} primary beam at 27 MeV and intensity ~ 150 pnA. The primary beam was directed onto a ^{2}H gas target at a pressure of 1217 mbar and a temperature of 93 K, corresponding to an effective thickness of 2 mg/cm^{2}.

A parallel plate avalanche counter (PPAC) was placed downstream 88 cm before the secondary target to monitor the beam and trigger the electronics. The energy of the secondary beam was 18.9 MeV after the PPAC and 18.5 MeV in the middle of the secondary target with intensity 4×10^{5} pps. Beam purity optimization was achieved by recording the energy spectrum of the secondary beam in different Si detectors placed across the EXOTIC beam line. For most of the runs the ^{7}Li contaminant beam was reduced below 4% by appropriate handling of the 30° bending magnet and the Wien filter.

The experimental setup included six telescopes from the EXOTIC detector array [22] located in symmetrical positions around the beam at $27 \pm 15°$, $69 \pm 15°$ and $111 \pm 15°$. Due to the limited beam time available only the four more forward telescopes registered significant counts. Each telescope comprised ΔE and E double-sided silicon strip detectors, with thicknesses of $\sim 55\,\mu$m and $300\,\mu$m, respectively, and active areas 64×64 mm^{2} with 32 strips per side, orthogonally oriented to define 2×2 mm^{2} pixels. Details of the handling of the detector signals can be found in ref. [22]. At the beam energy presented here, the elastically scattered ejectiles were stopped in the first stage of the telescope. Alpha particles were discriminated by the ΔE-E technique but are not considered in our analysis as a large number of them originate from beam contaminants (reactions on the primary target). The telescopes were fixed at a distance of ~ 11 cm from the target position, covering a total solid angle of 1.7 sr. The strips were short-circuited two by two, therefore the angular resolution is in principle $\sim 2°$ per angular position, considering a point-like beam spot on target. However, taking into account that the beam spot should have a diameter of ~ 10 mm according to previous studies [23] and the finite dimensions of a "double" strip, the actual angular resolution is estimated to be at most 5°. A 1.5 mg/cm^{2} thick ^{90}Zr target was installed on the target ladder at the centre of the target chamber, perpendicular to the beam. A 2 mg/cm^{2} thick ^{208}Pb target was installed on the same ladder and was used in a subsequent run to deduce the solid angle by assuming that the elastic scattering over the whole angular range was Rutherford.

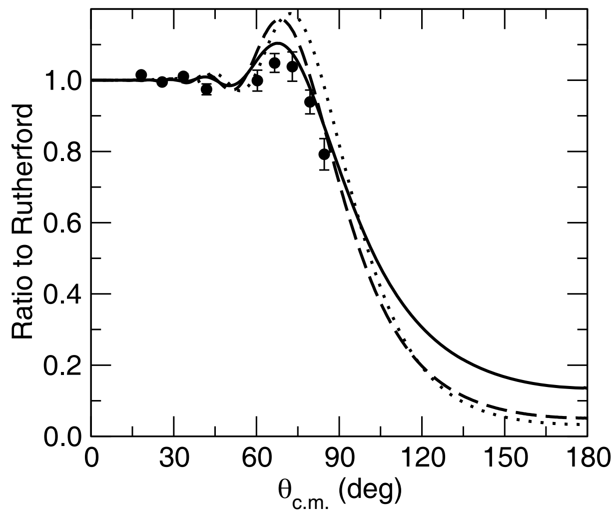

Fig. 1. Calculated quasi-elastic scattering angular distributions for 18.5 MeV ^{8}Li + ^{90}Zr compared with the data. The dotted, dashed and solid curves denote the no-coupling, CC and CRC calculations, respectively, see text for details. Note the linear cross section scale.

The measured quasi-elastic scattering angular distribution is presented in fig. 1. The data are quasi-elastic since inelastic scattering to the 0.98 MeV ^{8}Li 1^{+}_{1} and 2.19 MeV ^{90}Zr 2^{+}_{1} states could not be resolved from the elastic scattering peak. Due to the low statistics and taking into account the angular resolution of $\sim 5°$, the differential cross sections appearing in fig. 1 are the weighted means over each group of three scattering angles. It should also be noted that although the data obtained in this work are for quasi-elastic scattering rather than pure elastic, this does not affect our results since according to coupled channels calculations the difference between elastic and quasi-elastic scattering is within the experimental uncertainties for the range of angles where we have data. The same result was found for ^{8}Li + ^{208}Pb quasi-elastic scattering at near-barrier energies in ref. [2].

3 The calculations

The calculations were based on a "bare" ^{8}Li + ^{90}Zr optical potential with a double-folded real part and an "interior" Woods-Saxon imaginary part. The parameters of the Woods-Saxon imaginary part were: $W = 50\,\mathrm{MeV}$, $R = 1.0 \times (8^{1/3} + 90^{1/3})\,\mathrm{fm}$, $a = 0.3\,\mathrm{fm}$. The double-folded real part was calculated using the code DFPOT [24] and the energy-independent form of the M3Y effective nucleon-nucleon interaction given in ref. [25], with ^{90}Zr and ^{8}Li nuclear matter densities calculated according to the liquid drop model of Myers [26] and the prescription of ref. [27], respectively. Inelastic coupling potentials were obtained by numerically deforming the diagonal potential and projecting by Gaussian quadrature onto the required multipoles; imaginary coupling potentials were not included since due to the use of an "interior" imaginary potential their effect is negligible. All reaction calculations were performed with the code FRESCO [28].

Initial calculations included couplings to inelastic excitations of the bound 1^+ first excited state of ^{8}Li and the 2^+_1 and 3^-_1 states of ^{90}Zr only. The ^{8}Li coupling was treated within the rotational model, assuming that the 2^+ ground state and 0.98 MeV 1^+ state form part of a $K = 1$ rotational band, with a $B(E2; 2^+_1 \to 1^+_1)$ value of $55\,\mathrm{e^2\,fm^4}$, taken from a Coulomb excitation measurement [29], and a nuclear deformation length $\delta_2 = 2.4\,\mathrm{fm}$, obtained by re-fitting the ^{8}Li + ^{12}C inelastic scattering data of ref. [30]. The ^{90}Zr couplings were treated as single phonon excitations with $B(E2; 0^+_1 \to 2^+_1)$ and $B(E3; 0^+_1 \to 3^-_1)$ values from refs. [31] and [32], respectively, and nuclear deformation lengths $\delta_2 = 0.43\,\mathrm{fm}$ and $\delta_3 = 0.69\,\mathrm{fm}$ obtained by re-fitting the ^{6}Li + ^{90}Zr inelastic scattering data of ref. [33].

Couplings to the ^{90}Zr(^{8}Li, ^{7}Li)^{91}Zr and ^{90}Zr(^{8}Li, ^{9}Be)^{89}Y transfer reactions were then added within the CRC framework with full complex remnant terms and non-orthogonality corrections. The ^{7}Li + ^{91}Zr exit channel potential was calculated using the global parameters of Cook [34] while the ^{9}Be + ^{89}Y exit channel potential was the 26.7 MeV set of table II of ref. [35]. Stripping to the $3/2^-$ ground and $1/2^-$ first excited states of ^{7}Li and pickup to the $3/2^-$ ground state of ^{9}Be were included. Ground state reorientation and excitation of the first excited state in ^{7}Li were included in the ^{7}Li + ^{91}Zr exit channel with the $B(E2; 3/2^- \to 1/2^-)$ from ref. [36] and the nuclear deformation length $\delta_2 = 2.4\,\mathrm{fm}$ obtained by re-fitting the ^{7}Li + ^{90}Zr inelastic scattering data of ref. [37]. The $3/2^-$ and $1/2^-$ states were assumed to be members of a $K = 1/2$ rotational band. No inelastic couplings were included in the ^{9}Be + ^{89}Y exit channel. Spectroscopic factors for the $\langle ^8\mathrm{Li} | ^7\mathrm{Li} + n \rangle$ and $\langle ^9\mathrm{Be} | ^8\mathrm{Li} + p \rangle$ overlaps were from refs. [19] and [38], respectively. The transferred nucleons were bound in Woods-Saxon wells with radius and diffuseness parameters $r_0 = 1.25\,\mathrm{fm}$ and $a = 0.52\,\mathrm{fm}$ and $r_0 = 1.25\,\mathrm{fm}$ and $a = 0.65\,\mathrm{fm}$ for the $\langle ^8\mathrm{Li} | ^7\mathrm{Li} + n \rangle$ and $\langle ^9\mathrm{Be} | ^8\mathrm{Li} + p \rangle$ overlaps, respectively, with spin-orbit components of Thomas form and the same geometry. The depths of the central parts were adjusted to obtain the corresponding binding energies. The $\langle ^{91}\mathrm{Zr} | ^{90}\mathrm{Zr} + n \rangle$ overlaps (spectroscopic factors and neutron binding potentials) were from ref. [39], with couplings to all levels with $\mathrm{C^2S} \geq 0.10$ included. The $\langle ^{90}\mathrm{Zr} | ^{89}\mathrm{Y} + p \rangle$ overlaps were from ref. [40] with couplings to all four observed states in ^{89}Y included.

4 Results and discussion

In fig. 1 we compare the calculations with the data. We plot the results for quasi-elastic scattering including excitation of the ^{8}Li 1^+_1 and ^{90}Zr 2^+_1 states since these were not resolved from the elastic scattering in the measurement, although the contribution from the ^{90}Zr 2^+_1 state is negligible. Both inelastic excitation of the ^{90}Zr target states and coupling to the ^{90}Zr(^{8}Li, ^{9}Be)^{89}Y pickup reaction had a negligible effect on the calculated (quasi) elastic scattering. We emphasise that the calculations are not fits and do not include any adjustable parameters in the usual sense, all values being taken from the literature or from fits to other data sets. In this context the description of the data is good. The total reaction cross section (σ_R) obtained from the full calculation is 529 mb; an optical model fit to the quasi-elastic scattering data gives a value of $514 \pm 30\,\mathrm{mb}$ [20] (there will be a slight systematic error in this value due to the data being quasi-elastic rather than pure elastic, but the calculations presented here suggest that it will be within the experimental uncertainty). The dominant direct reaction contributions to σ_R are excitation of the ^{8}Li 1^+_1 state and the ^{90}Zr(^{8}Li, ^{7}Li)^{91}Zr stripping reaction, contributions from the other channels being negligible.

In fig. 2 we compare the results of the calculations for 18.5 MeV ^{8}Li + ^{90}Zr quasi-elastic scattering with similar calculations for 18.9 MeV ^{6}Li + ^{90}Zr elastic scattering and 18.5 MeV ^{7}Li + ^{90}Zr quasi-elastic scattering. The slightly higher incident energy for the ^{6}Li + ^{90}Zr system was to enable comparison with existing elastic scattering data [41] and does not affect significantly the discussion. Likewise, since ^{6}Li has no bound excited states and the contribution of the ^{90}Zr 2^+_1 state to the quasi-elastic scattering is negligible quasi-elastic and elastic scattering for ^{6}Li are indistinguishable here. The ^{6,7}Li calculations were similar to those for ^{8}Li. Double-folded real potentials were used in the entrance channels, the ^{6}Li nuclear matter density being derived from the empirical charge density of [42], suitably corrected for the charge distributions of the proton and neutron [25] and assuming that the proton and neutron densities were equal, while the ^{7}Li density was taken from ref. [43]; the ^{90}Zr nuclear matter density was again that of Myers [26]. Couplings to inelastic excitations of the ^{90}Zr 2^+_1 and 3^-_1 states were included using the

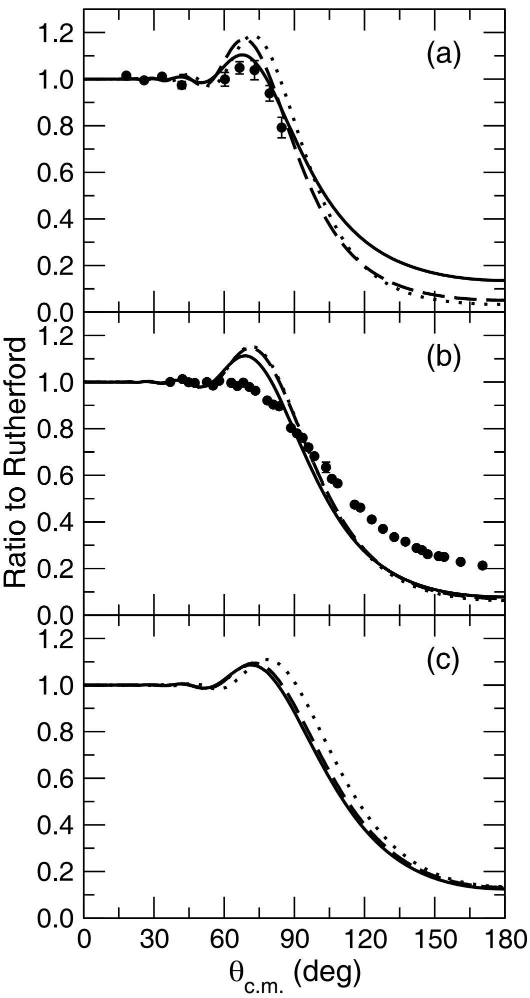

Fig. 2. (a) Quasi-elastic scattering angular distributions for 18.5 MeV ^{8}Li + ^{90}Zr, as in fig. 1. (b) Elastic scattering angular distributions for 18.9 MeV ^{6}Li + ^{90}Zr. Filled circles denote the data of ref. [41]. (c) Quasi-elastic scattering angular distributions for 18.5 MeV ^{7}Li + ^{90}Zr. Dotted, dashed and solid curves denote no-coupling, CC and CRC calculations, respectively, see text for details.

same $B(E)$ and δ values as for the ^{8}Li calculations. The ^{7}Li + ^{90}Zr calculations also included ground state reorientation and excitation of the first excited state in ^{7}Li using the same $B(E2)$ and δ_2 values as described previously for the ^{8}Li calculations.

The CRC calculations for both ^{6,7}Li + ^{90}Zr included couplings to the single neutron stripping reactions, with exit channel ^{5}Li + ^{91}Zr and ^{6}Li + ^{91}Zr optical potentials calculated using the global ^{6}Li parameters of Cook [34]. Stripping to the $3/2_1^-$ and $1/2_1^-$ resonances of ^{5}Li and the 1^+ ground state and 3_1^+ resonance of ^{6}Li were included, with spectroscopic factors taken from ref. [38], the transferred neutrons being bound in Woods-Saxon wells with radius and diffuseness parameters $r_0 = 1.25$ fm and $a = 0.65$ fm with spin-orbit components of Thomas form with the same geometry and depths of 6 MeV, the depths of the central parts being adjusted to give the correct binding energy. Form factors for the $\langle ^{91}\mathrm{Zr}|^{90}\mathrm{Zr} + n\rangle$ overlaps were as described previously. The ^{6}Li $1_1^+ \longleftrightarrow 3_1^+$ coupling was included in the ^{6}Li + ^{91}Zr exit channel but had no influence on the coupling effect on the elastic scattering.

The results presented in fig. 2 make it readily apparent that single neutron stripping coupling is much more important for ^{8}Li than for either ^{6}Li or ^{7}Li; for ^{7}Li its effect is negligible and for ^{6}Li it is confined to a relatively small reduction of the Coulomb-nuclear interference peak, whereas for ^{8}Li there are large effects both at backward angles and in the vicinity of the Coulomb-nuclear interference peak. The effect of coupling to inelastic excitation of the first excited state is similar for ^{8}Li and ^{7}Li, probably reflecting their similar nuclear deformation lengths. Since none of these calculations include couplings to breakup, known to be important for ^{6}Li and ^{7}Li (see, *e.g.*, [44]), one would not *a priori* expect them to describe the elastic scattering data. However, despite a comparable breakup threshold (2.03 MeV for $^{8}\mathrm{Li} \to {}^{7}\mathrm{Li} + n$ breakup compared to 1.47 MeV for $^{6}\mathrm{Li} \to \alpha + d$ and 2.47 MeV for $^{7}\mathrm{Li} \to \alpha + t$ breakup) a satisfactory description of the ^{8}Li + ^{90}Zr quasi-elastic scattering data is obtained *without* including breakup couplings, although further data at backward angles would be required to confirm this. Data for ^{7}Li + ^{90}Zr elastic scattering at 18.5 MeV are also desirable to complete the comparison.

5 Summary and conclusions

New data for ^{8}Li+^{90}Zr quasi-elastic scattering at the near-barrier energy of 18.5 MeV were adequately described by CRC calculations including couplings to excitations of the ^{8}Li 1_1^+ and ^{90}Zr 2_1^+ and 3_1^- excited states and the ^{90}Zr(^{8}Li,^{7}Li)^{91}Zr and ^{90}Zr(^{8}Li,^{9}Be)^{89}Y transfer reactions. Thus, in contrast to similar data for ^{6}Li + ^{90}Zr [41], breakup couplings appear to play a relatively minor rôle for ^{8}Li elastic scattering from this medium mass target. Coupling to the single neutron stripping reaction has an important effect on the ^{8}Li + ^{90}Zr (quasi) elastic scattering at this energy, unlike ^{6,7}Li + ^{90}Zr where the influence of this coupling is small. This is by no means a trivial result, as a naïve comparison of the S_n values would suggest. The integrated cross sections for single neutron stripping induced by ^{8}Li, ^{7}Li and ^{6}Li are 61.6 mb, 26.3 mb and 60.3 mb, respectively, (the ^{6}Li value is for an incident energy of 18.5 MeV to enable a fair comparison) so that one might expect single neutron stripping to have a similar importance for ^{6}Li, which fig. 2 shows is clearly not the case. The Q values are more relevant to this question than the S_n values and these are: +5.16 MeV, −0.06 MeV and +1.53 MeV for ^{90}Zr(^{8}Li,^{7}Li), ^{90}Zr(^{7}Li,^{6}Li) and ^{90}Zr(^{6}Li,^{5}Li), respectively. While they help to explain the variations of the cross sections —it will be recalled that the optimum Q value for neutron transfer is 0 MeV— they do not explain the much smaller coupling effect seen for ^{6}Li which must be ascribed to detailed differences in the nuclear structure of the Li isotopes.

While our calculations are parameter free in the conventional sense choices were made for some inputs which have an influence on the result. The most important of these is the use of the ^{8}Li nuclear matter density of Bhagwat *et al.* [27]. Other ^{8}Li densities are available in the literature, *e.g.*, those of Fan *et al.*[45] and Dobrovolsky *et al.* [46], and these give a slightly worse description of the data when used to calculate the double-folded real potential (alternative ^{90}Zr densities had negligible influence). The four different forms of ^{8}Li density given by Dobrovolsky *et al.*[46] give similar results to each other and to the density of Fan *et al.* [45]; this merely reflects their similar rms matter radii, the density of Bhagwat *et al.* [27] giving a somewhat larger value, suggesting a preference for a more attractive nuclear potential in the nuclear surface. The influence of single neutron stripping coupling on the (quasi) elastic scattering is not affected by the choice of ^{8}Li matter density.

In summary, the conclusion that breakup coupling effects are weaker for ^{8}Li than for ^{6}Li and ^{7}Li remains to be confirmed, both by extending the current ^{8}Li (quasi) elastic scattering angular distribution to larger angles and the measurement of new data for $^7\mathrm{Li} + {}^{90}\mathrm{Zr}$ elastic scattering at 18.5 MeV. However, the much stronger influence of single neutron stripping coupling on the (quasi) elastic scattering for ^{8}Li is a robust conclusion, unaffected by the choice of input parameters to the calculations. It is once again seen that near-barrier elastic scattering can probe quite subtle differences in nuclear structure.

This work was partly funded by the European Union Seventh Framework Programme FP7/2007-2013 under Grant Agreement No. 262010-ENSAR.

References

1. N. Keeley *et al.*, Prog. Part. Nucl. Phys. **63**, 396 (2009).
2. E.F. Aguilera *et al.*, Phys. Rev. C **63**, 061603 (2001).
3. A. Di Pietro *et al.*, Phys. Rev. C **69**, 044613 (2004).
4. A. Pakou *et al.*, Phys. Rev. C **76**, 054601 (2007).
5. A. Pakou *et al.*, Eur. Phys. J. A **39**, 187 (2009).
6. A. Di Pietro *et al.*, Phys. Rev. Lett. **105**, 022701 (2010).
7. A. Di Pietro *et al.*, Phys. Rev. C **85**, 054607 (2012).
8. T. Druet, P. Descouvemont, Eur. Phys. J. A **48**, 147 (2012).
9. N. Keeley *et al.*, Phys. Rev. C **82**, 034606 (2010).
10. E.F. Aguilera *et al.*, Phys. Rev. C **79**, 021601 (2009).
11. J. Lubian *et al.*, Phys. Rev. C **79**, 064605 (2009).
12. N. Keeley, R.S. Mackintosh, C. Beck, Nucl. Phys. A **834**, 792c (2010).
13. M.Y. Lee *et al.*, Nucl. Instrum. Methods Phys. Res. A **422**, 536 (1999).
14. F. Farinon *et al.*, Nucl. Instrum. Methods B **266**, 4097 (2008).
15. A. Lépine-Szily, R. Lichtenthäler, V. Guimarães, Eur. Phys. J. A **50**, 128 (2014).
16. F.D. Becchetti *et al.*, Phys. Rev. C **40**, R1104 (1989).
17. F.D. Becchetti *et al.*, Phys. Rev. C **48**, 308 (1993).
18. J.J. Kolata *et al.*, Phys. Rev. C **65**, 054616 (2002).
19. A.M. Moro *et al.*, Phys. Rev. C **68**, 034614 (2003).
20. A. Pakou *et al.*, Eur. Phys. J. A **51**, 55 (2015).
21. M. Mazzocco *et al.*, Nucl. Instrum. Methods B **266**, 4665 (2008).
22. E. Strano *et al.*, Nucl. Instrum. Methods B **317**, 657 (2013).
23. A. Pakou *et al.*, Phys. Rev. C **87**, 014619 (2013).
24. J. Cook, Comput. Phys. Commun. **25**, 125 (1982).
25. G.R. Satchler, W.G. Love, Phys. Rep. **55**, 183 (1979).
26. W.D. Myers, Nucl. Phys. A **145**, 387 (1970).
27. A. Bhagwat, Y.K. Gambhir, S.H. Patil, Eur. Phys. J. A **8**, 511 (2000).
28. I.J. Thompson, Comput. Phys. Rep. **7**, 167 (1988).
29. J.A. Brown *et al.*, Phys. Rev. Lett. **66**, 2452 (1991).
30. R.J. Smith *et al.*, Phys. Rev. C **43**, 2346 (1991).
31. S. Raman, C.W. Nestor, Jr., P. Tikkanen, At. Data Nucl. Data Tables **78**, 1 (2001).
32. T. Kibédi, R.H. Spear, At. Data Nucl. Data Tables **80**, 35 (2002).
33. D.J. Horen *et al.*, Phys. Rev. C **47**, 629 (1993).
34. J. Cook, Nucl. Phys. A **388**, 153 (1982).
35. C.S. Palshetkar *et al.*, Phys. Rev. C **89**, 064610 (2014).
36. A. Weller *et al.*, Phys. Rev. Lett. **55**, 480 (1985).
37. R.J. Puigh, K.W. Kemper, Nucl. Phys. A **313**, 363 (1979).
38. S. Cohen, D. Kurath, Nucl. Phys. A **101**, 1 (1967).
39. D.K. Sharp *et al.*, Phys. Rev. C **87**, 014312 (2013).
40. G.J. Kramer, H.P. Blok, L. Lapikás, Nucl. Phys. A **679**, 267 (2001).
41. H. Kumawat *et al.*, Phys. Rev. C **78**, 044617 (2008).
42. L.R. Suelzle, M.R. Yearian, H. Crannell, Phys. Rev. **162**, 992 (1967).
43. J. Cook *et al.*, Phys. Rev. C **27**, 1536 (1983).
44. Y. Sakuragi, M. Yahiro, M. Kamimura, Prog. Theor. Phys. Suppl. **89**, 136 (1986).
45. G.W. Fan *et al.*, Phys. Rev. C **90**, 044321 (2014).
46. A.V. Dobrovolsky *et al.*, Nucl. Phys. A **766**, 1 (2006).